^{124}I PET-Based 3D-RD Dosimetry for a Pediatric Thyroid Cancer Patient: Real-Time Treatment Planning and Methodologic Comparison

Robert F. Hobbs[1], Richard L. Wahl[1], Martin A. Lodge[1], Mehrbod S. Javadi[1], Steve Y. Cho[1], David T. Chien[1], Marge E. Ewertz[2], Caroline E. Esaias[1], Paul W. Ladenson[2], and George Sgouros[1]

[1]Department of Radiology, Johns Hopkins University, Baltimore Maryland; and [2]Department of Endocrinology, Johns Hopkins University, Baltimore, Maryland

Patient-specific 3-dimensional radiobiologic dosimetry (3D-RD) was used for ^{131}I treatment planning for an 11-y-old girl with differentiated papillary thyroid cancer, heavy lung involvement, and cerebral metastases. ^{124}I PET was used for pharmacokinetics. Calculation of the recommended administered activity, based on lung toxicity constraints, was performed in real time (i.e., during the data-acquisition interval). The results were available to the physician in time to influence treatment; these estimates were compared with conventional dosimetry methodologies. In subsequent, retrospective analyses, the 3D-RD calculations were expanded to include additional tumor dose estimates, and the conventional methodologies were reexamined to reveal the causes of the differences observed. A higher recommended administered activity than by an S-value–based method with a favorable clinical outcome was obtained. This approach permitted more aggressive treatment while adhering to patient-specific lung toxicity constraints. A retrospective analysis of the conventional methodologies with appropriate corrections yielded absorbed dose estimates consistent with 3D-RD.

Key Words: oncology; radiobiology/dosimetry; radionuclide therapy; 3D-RD; dosimetry; PET; thyroid; treatment planning

J Nucl Med 2009; 50:1844–1847
DOI: 10.2967/jnumed.109.066738

Since the 1990s, patient-specific 3-dimensional (3D)-imaging–based dosimetry has been an area of interest and ongoing development (*1*). To the extent that this dosimetry technique has been applied to patient studies, all applications have been retrospective. In this work, prospective or real-time implementation of an imaging-based Monte Carlo calculation using the 3D-RD dosimetry package (*2*) is illustrated for the radioiodine treatment of a pediatric thyroid cancer patient. Implementation of a 3D imaging–based patient-specific dosimetry methodology that can be performed in a timely and clinically relevant period—that is, one in which the results are available to the treating physician in time to help identify the optimal therapeutic activity administration—is important in selected, clinically challenging cases. The work also examines the related and important question of whether the mean absorbed dose values obtained by the highly patient-specific approach embodied by 3D-RD could have been arrived at by much simpler conventional and less logistically and monetarily costly methods.

The real-time aspect of the 3D-RD calculations took advantage of an algorithm design that allows dose calculations to start without the need for the complete dataset. This is accomplished by calculating the dose rate obtained from each scan at each time point and then integrating these over time after the last scan has been collected and processed. In this way, the time-intensive Monte Carlo calculations are performed during the interval between image acquisitions, and the more rapid integration over time is performed on the dose-rate images. In subsequent, retrospective analyses (i.e., after the real-time calculation was completed and the results provided to the treating physician), the 3D-RD calculations were expanded to include additional tumor dose estimates. The conventional methodologies were reexamined to clarify the causes of the differences observed with 3D-RD. The 3D-RD calculations also included secondary considerations such as radiobiologic modeling by incorporating the biologic effective dose (BED) and equivalent uniform dose (EUD) formalisms for several tumor sites.

Received Jun. 30, 2009; revision accepted Jul. 13, 2009.
For correspondence or reprints contact: George Sgouros, Department of Radiology, Johns Hopkins University, School of Medicine, CRB II 4M.61, 1550 Orleans St., Baltimore, MD 21231.
E-mail: gsgouros@jhmi.edu

MATERIALS AND METHODS

The methodology and results obtained are illustrated for an 11-y-old girl, presenting with metastatic papillary carcinoma after thyroidectomy. A diagnostic activity level of 122 MBq (3.3 mCi)

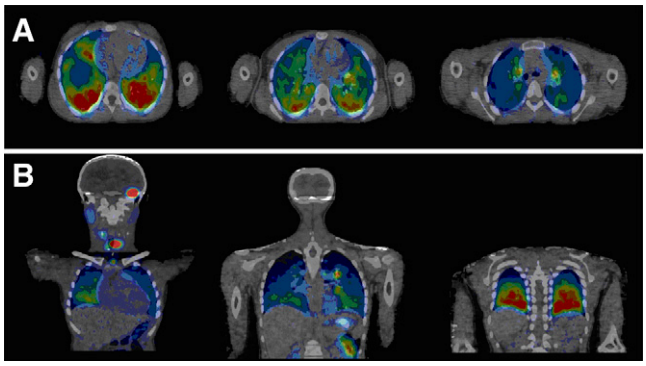

FIGURE 1. Selected fused ^{124}I PET/CT transverse (A) and coronal (B) views of lungs. Views depicted extend from base of diaphragm to vertex of skull.

of ^{131}I was administered at another medical center, where the whole-body scan revealed thyroid bed, bilateral lung, and intracranial foci of iodine-avid tissue.

Subsequently, the patient was emergently transferred to Johns Hopkins for further evaluation in anticipation of ^{131}I therapy. A repeated ^{131}I whole-body planar scan, without readministration of ^{131}I, confirmed the prior outside findings, and SPECT/CT scans of the head and neck revealed the intracranial uptake to represent bilateral temporal lobe brain metastases. Notably, the left temporal lobe brain metastasis had extremely high ^{131}I uptake, causing significant scatter and SPECT reconstruction artifacts. MRI of the brain confirmed 2 lesions in the temporal lobes bilaterally, with the lesion on the left measuring $2.4 \times 2.0 \times 1.9$ cm^3 and the lesion on the right measuring $0.8 \times 0.9 \times 0.8$ cm^3. Baseline pulmonary function tests showed both obstructive and restrictive lung defects; thyroglobulin laboratory results showed a concentration of 9,553 ng/mL.

Because the high retention of previously administered ^{131}I would affect and significantly complicate ^{131}I dosimetry measurements, PET-based ^{124}I dosimetry was pursued to define the optimally effective and safe ^{131}I therapeutic administered activity. After parental consent was obtained, the patient was administered a diagnostic activity of 92.5 MBq (2.5 mCi capsule) of ^{124}I-NaI (IBA Molecular North America). Figure 1 shows fused PET/CT images at 24 h. The ^{124}I was administered on a compassionate basis after consultation with the U.S. Food and Drug Administration and the Johns Hopkins internal review board.

Details regarding the imaging and dosimetry methodologies are available in the supplement to this article (supplemental materials are available online only at http://jnm.snmjournals.org).

RESULTS

Real-Time 3D-RD Calculation

The administered activity predicted to deliver the maximum tolerated dose of 27 Gy to the lung volume of interest (VOI) (*3*), considered as a whole, was 5.11 GBq (138 mCi) of ^{131}I.

OLINDA/Whole-Organ S-Value–Based Calculation

To best approximate the lung-to-lung S value for the treated patient, the S values already tabulated in OLINDA were interpolated to match the whole-body weight of the patient. For this patient, who had a whole-body mass of 37 kg, calculation using the interpolated S value gave an absorbed dose of 8.59 mGy/MBq or 3.14 GBq (85 mCi) of administered activity to deliver 27 Gy to the lungs considered as a whole (i.e., including tumor).

Benua–Leeper Calculation

The lung toxicity constraint based on total-body activity at 48 h gave a recommended administered activity of 8.17 GBq (220 mCi). The bone marrow toxicity constraint, calculated from a limit of 2 Gy to blood, was 5.60 GBq (151 mCi).

Detailed results for each of these dosimetry methods are provided in the supplement.

After considering the OLINDA, Benua–Leeper (*4*), and 3D-RD estimates, and the assumptions used to arrive at each estimate, the treating physician prescribed 5.11 GBq. As per schedule, the patient was administered 5 GBq 1 wk after tracer injection. The fit parameters from the 3D-RD calculation for the therapeutic quantities to the lungs and tumors are given in Supplemental Table 2; because of time constraints in these real-time calculations, no effort was made to discriminate between tumor in the lungs and normal lungs.

Retrospective 3D-RD Dosimetry

The 3D-RD dosimetry calculations were expanded to examine tumor absorbed dose after the real-time calculations were completed and the patient was treated. Retrospective 3D-RD absorbed dose calculations were performed for all of the distinct tumor lesions, tumor in the lungs, and normal lungs. A summary of mean absorbed dose, BED, and EUD results is given in Table 1. The vox subscript refers to mean values obtained by averaging the absorbed dose to individual voxel values; quantities with no subscript represent mean doses over the whole VOI (i.e., the cumulated activity is assigned to the whole volume, and the dose calculation is for the volume taken as a whole).

TABLE 1. 3D-RD Absorbed Dose (D), BED, and EUD Results for Different Tumors and for Normal Lung Tissue

	Normal	Tumor				
Category	lung	Lung	L brain	R brain	Sternum	Thyroid
D	—	—	986	142	30.6	33.5
BED	—	—	1270	149	30.8	34.8
D_{vox}	20.2	42.1	834	132	27.9	41.0
BED_{vox}	23.1	43.2	1220	142	28.1	42.8
EUD	21.2	23.0	89.1	55.9	10.4	9.0

Vox subscript indicates average voxelized results, whereas absence of subscript refers to results of VOI considered as whole; consequently, there are no results for segmented VOI lung tissues (normal lung vs. lung tumor) as they do not exist separately but form single lung VOI.

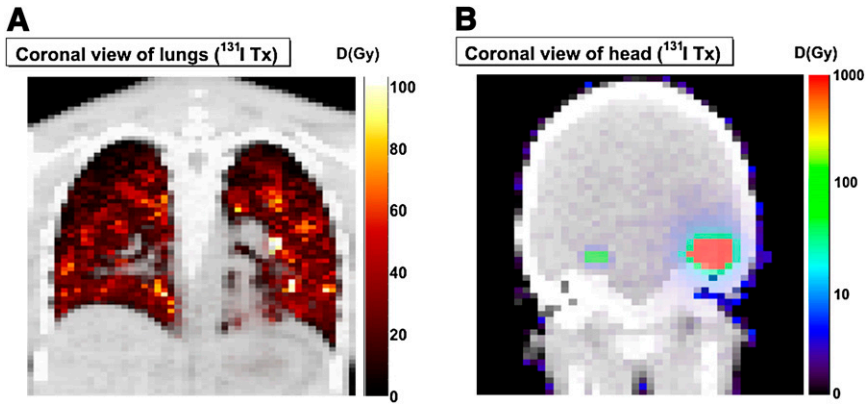

FIGURE 2. Representative coronal slices of absorbed dose (D) maps of 2 different datasets: torso (measured) (A) and head (modeled) (B). In modeled calculation, average tumor activity concentration was placed in 2 tumor-associated VOIs defined using CT; voxels representing normal brain were assigned average (background) brain activity concentration. 3D-RD was then executed using these 2 as source regions of uniform activity irradiating normal brain. In this way, possible calculation artifacts associated with high tumor count–density gradients were avoided. Both images are viewed anteriorly.

The absorbed dose to normal brain overall and also brain regions adjacent to the 2 brain tumors was also calculated. The maximum absorbed dose in a single voxel of normal brain tissue is 65.6 Gy, whereas the average absorbed dose is 0.95 Gy. Only 9 voxels (of 76,437; i.e., 0.012%) had doses greater than 50 Gy, and only 101 (0.13%) had doses greater than 20 Gy.

Figure 2 shows selected coronal slices of the absorbed dose maps created by 3D-RD, with accompanying color scales. The torso has a linear scale and shows the results from the measured activities, and the head has a logarithmic scale and shows the results of the model, created for purposes of normal brain toxicity evaluation.

By improving the patient specificity of the OLINDA and Benua–Leeper methodologies using information obtained as a result of the 3D-RD analysis, the recommended administered activity to deliver no more than 27 Gy to the lungs from the conventional approaches was within 2% of the 3D-RD values; these are summarized in Table 2.

Further details for the 3D-RD retrospective dosimetry results and the conventional dosimetry reexamination are provided in the online supplement.

DISCUSSION

Clinical Outcome

The patient experienced no pulmonary, neurologic, or other adverse clinical response to ^{131}I treatment. Twelve months after radioiodine treatment, the patient's serum thyroglobulin level after comparable thyroid hormone withdrawal had declined from its pretreatment level, 9,553 ng/mL to 777 ng/mL (−92%). The left and right lobe metastatic lesions had decreased from their respective pretreatment largest diameters, 24 and 9 mm, to 5 and less than 1 mm.

TABLE 2. Recommended Administered Activities for Estimated 27 Gy to Lung VOI as Determined by Different Methodologies

	Administered activities (GBq)		
Method	3D-RD	S value (OLINDA)	Benua–Leeper
Prospective	5.11	3.14	8.17
Retrospective	5.11	5.16	5.17

Retrospective S-value method used lung mass rather than body mass as parameter; retrospective Benua–Leeper calculation followed DRC methodology (*7*).

Posttherapy Results

Given the available imaging resolution, discrimination between normal tissue and lung tissue is difficult if not impossible and can give only an idea of the delineation for what are most likely micrometastases smaller than the resolution of the detector (*5*). A highly desirable possible consideration for future treatment planning would be to discriminate the voxels for tissue type in advance and scale the therapeutic activity to deliver the limiting dose only to the defined normal lung tissue voxels, considered together as healthy lung. Clinically, limiting the dose to normal lung to tolerable levels is the most concerning issue in treatment planning; as such, the discrimination between tumor and normal lung voxels is less about the definition of tumor than about the definition of healthy lung. In our present case, with our first-order discrimination, this would have translated as recommending an administered activity of 6.83 GBq (185 mCi) as opposed to 5.11 GBq.

The average dose to brain tissue as shown in the brain model is relatively small, but the maximum voxel absorbed dose is 65.6 Gy. This value is slightly above the generally accepted 50- to 60-Gy threshold for gray matter toxicity (*6*), whereas most voxels are significantly lower.

Method Comparison

This case illustrates the discrepancies that can occur between results arrived at by different methodologies designed to calculate the same quantity—in this case, the maximum administered activity tolerated by the lungs. From 3.14 GBq for an S-value–based method to 8.17 GBq for the traditional Benua–Leeper method, a factor of 2.6 was observed.

However, the results from the dose-rate constraint (DRC) adaptation (described in the online supplemental material) of the Benua–Leeper method show a value much closer to that from 3D-RD (5.16 GBq), and the OLINDA S-value method also gave a similar result after compensating for lung mass (5.17 GBq). This convergence of values has to be reassuring from a clinical standpoint: it suggests that as long as the chosen method is implemented correctly, the outcomes are far more comparable. This study also highlights the potential gains in implementing a more detailed analysis. Appropriate (i.e., effective lung mass–based) correction of the OLINDA S value would not have ordinarily been considered without the CT-based analysis of total lung mass needed for the initial, real-time 3D-RD calculation.

A discussion on the interpretation of EUD and BED and also additional discussion on the importance of partial-volume corrections on quantification and the delineation of normal lung from tumor voxels may be found in the online supplemental material.

CONCLUSION

Real-time treatment planning using 3D-RD has been demonstrated in a difficult pediatric thyroid case involving lung metastases. Sequential ^{124}I PET/CT studies allowed dosimetry planning even in the case of ^{131}I present systemically. A straightforward implementation of simpler, alternative approaches gave results substantially different from those obtained using 3D-RD. With appropriate corrections, however, the simpler alternative methodologies gave values similar to those obtained with 3D-RD; however, the needed corrections would not necessarily have been known if the 3D-RD analysis had not been performed for this patient. The 3D-RD analysis also provided more detailed information regarding potential efficacy and toxicity.

ACKNOWLEDGMENT

This work was partially supported by grant NIH.R01 CA116477.

REFERENCES

1. Sgouros G, Frey E, Wahl R, He B, Prideaux A, Hobbs R. Three-dimensional imaging-based radiobiological dosimetry. *Semin Nucl Med.* 2008;38:321–334.
2. Prideaux AR, Song H, Hobbs RF, et al. Three-dimensional radiobiologic dosimetry: application of radiobiologic modeling to patient-specific 3-dimensional imaging-based internal dosimetry. *J Nucl Med.* 2007;48:1008–1016.
3. Press OW, Eary JF, Appelbaum FR, et al. Radiolabeled-antibody therapy of B-cell lymphoma with autologous bone marrow support. *N Engl J Med.* 1993;329:1219–1224.
4. Benua R, Leeper R. A method and rationale for treating metastatic thyroid carcinoma with the largest safe dose of ^{131}I. In: Medeiros-Neta GE, Gaitan E, eds. *Frontiers in Thyroidology.* New York, NY: Plenum Medical; 1986:1317–1321.
5. Freudenberg LS, Jentzen W, Muller SP, Bockisch A. Disseminated iodine-avid lung metastases in differentiated thyroid cancer: a challenge to ^{124}I PET. *Eur J Nucl Med Mol Imaging.* 2008;35:502–508.
6. Steen RG, Koury BSM, Granja CI, et al. Effect of ionizing radiation on the human brain: white matter and gray matter T1 in pediatric brain tumor patients treated with conformal radiation therapy. *Int J Radiat Oncol Biol Phys.* 2001;49:79–91.
7. Sgouros G, Song H, Ladenson PW, Wahl RL. Lung toxicity in radioiodine therapy of thyroid carcinoma: development of a dose-rate method and dosimetric implications of the 80-mCi rule. *J Nucl Med.* Dec 2006;47:1977–1984.

JNM The Journal of NUCLEAR MEDICINE

^{124}I PET-Based 3D-RD Dosimetry for a Pediatric Thyroid Cancer Patient: Real-Time Treatment Planning and Methodologic Comparison

Robert F. Hobbs, Richard L. Wahl, Martin A. Lodge, Mehrbod S. Javadi, Steve Y. Cho, David T. Chien, Marge E. Ewertz, Caroline E. Esaias, Paul W. Ladenson and George Sgouros

J Nucl Med. 2009;50:1844-1847.
Published online: October 16, 2009.
Doi: 10.2967/jnumed.109.066738

The Journal of Nuclear Medicine is published monthly.
SNMMI | Society of Nuclear Medicine and Molecular Imaging
1850 Samuel Morse Drive, Reston, VA 20190.
(Print ISSN: 0161-5505, Online ISSN: 2159-662X)

SNMMI SOCIETY OF NUCLEAR MEDICINE AND MOLECULAR IMAGING